

Fair contrastive pre-training for geographic image segmentation

Miao Zhang
New York University
miaozhng@nyu.edu

Rumi Chunara
New York University
rumi.chunara@nyu.edu

Abstract

Contrastive self-supervised learning is widely employed in visual recognition for geographic image data (remote or proximal sensing), but because of landscape heterogeneity, models can show disparate performance across spatial units. In this work, we consider fairness risks in such contrastive pre-training; we show learnt representations present large performance gaps across selected sensitive groups: urban and rural areas for satellite images and city GDP level for street view images on downstream semantic segmentation. We propose fair dense representations with contrastive learning (FairDCL) to address the issue, a multi-level latent space de-biasing objective, using a novel dense sensitive attribute encoding technique to constrain spurious local information disparately distributes across groups. The method achieves improved downstream task fairness and outperforms state-of-the-art methods for the absence of a fairness-accuracy trade-off. Image embedding evaluation and ablation studies further demonstrate effectiveness of FairDCL. As fairness in geographic imagery is a nascent topic without existing state-of-the-art data or results, our work motivates researchers to consider fairness metrics in such applications, especially reinforced by our results showing no accuracy degradation. Our code is at: <https://anonymous.4open.science/r/FairDCL-1283>

1. Introduction

Dense image predictions with deep learning for tasks such as segmentation have a variety of applications in landscape feature analysis from geographic images. Success of the methods rely on powerful visual representations that include both local and global feature information. However, since pixel-level annotations are costly, fully supervised learning is challenging when the amount and variety of labeled data is scarce. Thus, self-supervised learning is a promising alternative via pre-training a feature extractor and transferring learnt representations to downstream problems [10, 58]. Learning effective dense representations is therefore important to pixel-wise geographic image recog-

nition. So far, contrastive self-supervised techniques have shown state-of-the-art performance in learning satellite image representations for land cover semantic segmentation across locations [1, 44, 45, 64].

Recent work has highlighted performance inequities by geographic area [8, 28, 30, 47]. Therefore, alongside the increased potential of self-supervised contrastive learning, here we turn our attention to fairness risks in recognition outcomes from geographic images. Fairness is an increasingly important concern in vision understanding, considering its usage for societal decisions across many areas such as health, urban planning, climate change and disaster risk assessment [29, 30, 50]. Further, while recent work calls for more focus on fairness studies for imagery with human as objects [54], there is very limited fairness work on model performance disparities for remote sensing images despite their wide applications.

To bridge this gap, we examine model semantic segmentation prediction and identify disparities across geographic subgroups on satellite image and city street view datasets from three different locations. As previous work shows, segmentation can be inherently difficult for some geography types. For example, in areas where land-cover objects have higher density or heterogeneity [73], performance will be lower even with balanced data distribution. Moreover, identifying and thus addressing disparities for geographic object segmentation is different from fairness tasks in other image types such as facial images. First, facial recognition (mostly classification) relies on image-level global representations, which are not ideal for segmentation for which local features are important. Second, specifying sensitive attributes for geographic images is challenging because sensitive land-cover features are generally task-related, unlike many previous fairness studies where bias is easier to identify and separate out (e.g. skin color, gender) because the sensitive attributes are less relevant with respect to the specific task [21, 41, 62]. In sum, existing fairness methods do not always apply to geographic data and relevant tasks. Instead, we develop unbiased representation learning by relying on generalizable and robust landscape features,

while reducing spurious features that are unequally correlated with sensitive groups (referred to as *bias* or *sensitive information*). By constructing regularization terms on the statistical association between local features and sensitive variables within the encoder, the approach directly mitigates performance disparities in pixel-level semantic segmentation. Our specific contributions are:

- We propose a causal model depicting the relationship between image features and sensitive attributes to unravel the type of implicit bias caused by spurious correlations. It enables us to identify and address unique fairness challenges in geographic image recognition.
- For the described bias scenario, we design a multi-scale local fair representation learning method, termed FairDCL, which adapts conventional image-scale mutual information guided de-biasing onto dense visual representation and pixel-level applications.
- On three diverse geographic imagery datasets, FairDCL shows the representation advantages for contrastive pre-training; it surpasses state-of-the-art fairness methods with smaller group difference, has higher worst-case group performance, and does not sacrifice overall accuracy on downstream semantic segmentation tasks.

2. Related work

Contrastive learning for dense representation Contrastive learning is used as a self-supervised pre-training approach for various downstream vision tasks including classification, detection and segmentation [1, 4, 5, 15, 31, 42, 59]. Though most work in this area focuses on optimizing global representations for image-level tasks [4, 5, 66], recent work has turned to learning representations suitable for pixel-level predictions; Wang *et al.* [63] design a dense projection through local feature vectors for contrastive objectives, thus preserving spatial information. Xiong *et al.* [68] use overlapped local blocks to increase depth and capacity for decoders that improves local learning. Others [3, 34, 67] apply local contrastive loss to enlarge representation dissimilarities across regions and similarities across augmented views. Such methods show the importance of local features on dense visual problems like object detection and segmentation, which motivates method design in this study.

Fairness in vision Fairness-promoting approaches are being designed in multiple visual recognition domains. In face recognition applications, methods are proposed towards mitigating bias across groups such as by age, gender or race/ethnicity. Methods include constraining models from learning sensitive information by adversarially training sensitive attribute classifiers [32, 39], using penalty losses [46, 69], sensitive information disentanglement [7, 36], and augmenting biased data using generative networks [41]. These methods achieve fairer recognition, but

only focus on global classification tasks. Related to healthcare data and practice, Puyol-Antón *et al.* [38] improve cardiac MR segmentation by jointly training a racial meta-attribute classifier. Yuan *et al.* [70] reduce skin tone bias in skin disease classification and segmentation by altering colors in images but preserve lesion structure edges. Efforts on geographic imagery include achieving even class-level segmentation results on street scenes using tilted cross entropy loss [52] and fair underwater object detection by simulating better quality images for scarce species [9].

Limitations of existing fairness work in vision include (1) requiring prior knowledge on sensitive attribute properties, such as skin colors for ethnicity groups, which is not available in our task, nor is homogeneous, (2) mostly for classification built on image-level representation, whose achieved fairness would not necessarily extend to pixel-level dense predictions, (3) very little work on fairness for geographic images, for which biased features are harder to discover, interpret and remove, compared to facial images.

Fair contrastive learning Fairness has been less studied in contrastive approaches. Such work is needed, as shown by Sirotkin *et al.* [49], self-supervised models can incorporate implicit bias from data and potentially transfer to downstream tasks. A few recent studies pay the attention; Tsai *et al.* [55] propose sampling positive and negative pairs from the same group to restrict models from leveraging sensitive information, but could potentially lose task-specific information of the data contrasts with different groups. Park *et al.* [37] propose fairness-aware losses to penalize sensitive information used in positive and negative pair differentiation, but in a supervised setting with target labels fully available. The methods' increased downstream fairness scores and limited research in this area all motivate us to further explore fairer representations in contrastive learning.

Mutual information for de-biasing For de-biasing purposes, mutual information as a statistical association measure between variables [23] has recently been used to instruct training objectives to minimize model dependence on irrelevant variables. In deep networks, mutual information lower bound estimators are adapted, such as MINE [2] and DeepInfoMax [16]. Ragonesi *et al.* [40] use MINE loss to model optimization which shows utility in removing irrelevant information in digit and face classifications. Zhu *et al.* [76] compute cross-sample mutual information for reducing different bias variations. Previous work shows leveraging mutual information can ease the requirement of pre-defined bias properties between groups, which informs the de-biasing approach in this study on geographic imagery.

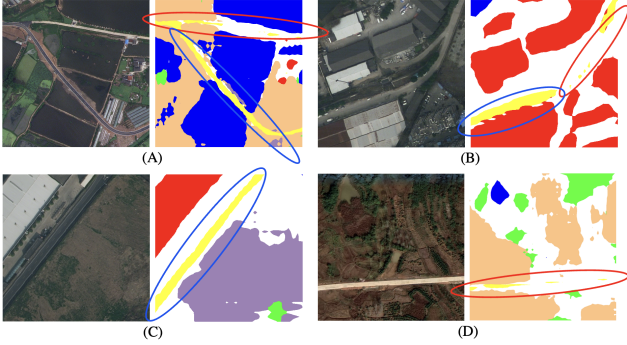


Figure 1. Examples of **Segmentation bias** due to spurious visual representation; the model segments certain road patterns well (blue circles), but segments the variations poorly (red circles).

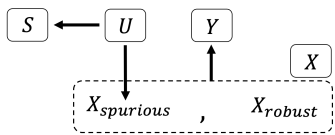


Figure 2. **Diagram of defined causal relationships** between representation X learnt with contrastive pre-training, target task prediction outputs Y , and sensitive attribute S . X contains two parts, $X_{spurious}$ generated from features spuriously correlated to sensitive attributes and X_{robust} generated from independent and unchangeable features. U is an unmeasured confounder which causes both S and $X_{spurious}$ thus result in correlations between S and $X_{spurious}$. Examples are discussed in Sec. 3.1.

3. Problem definition

3.1. Unfairness in satellite image recognition

Land-cover objects in satellite images often have heterogeneous shapes and distributions in urban and rural areas even within the same geographic region. These distributions are affected by varying levels of development (infrastructure, greening, etc). Considering an attribute $S = \{s_0, s_1\}$ denoting urban/rural area, we define visual representations learnt by the model encoder as $X = \{X_{spurious}, X_{robust}\}$, where $X_{spurious}$ includes information that varies across sensitive groups in S , for example, the contour, color, or texture of “Road” or “Building” class. X_{robust} , on the other hand, includes generalizable information, for example, “Road” segments are narrow and long, while “Building” segments are clustered. When model output Y is drawn from both X_{robust} and $X_{spurious}$, it can lead to biased performance. For example, roads in grey/blue color (Figure 1 A), with vehicles on them (Figure 1 B), and with lane markings (Figure 1 C), are segmented better (blue circle) than the others (red circle, Figure 1 D). Examples of more classes’ spurious and robust components are in the Supplementary Material A. As a result, urban and rural embedding containing disproportionate spurious information levels will cause group-level model performance dispari-

ties in semantic segmentation. This problem is sketched out, in terms of causal relationships, in Figure 2. Different from previous fair methods which directly remove sensitive information, which is not available in the problem we study, we define the fairness goal to be to remove spurious information from representations correlated to sensitive features. That is, to obtain \hat{X}_{robust} which promotes $\hat{Y} \perp S | \hat{X}_{robust}$. The instinctive fairness benefit of learning X_{robust} over $X_{spurious}$ is that it can relieve the need to expose a model to enough data to extract relevant target representations from non-generalizable feature variations, especially when the underrepresented group’s data is scarce.

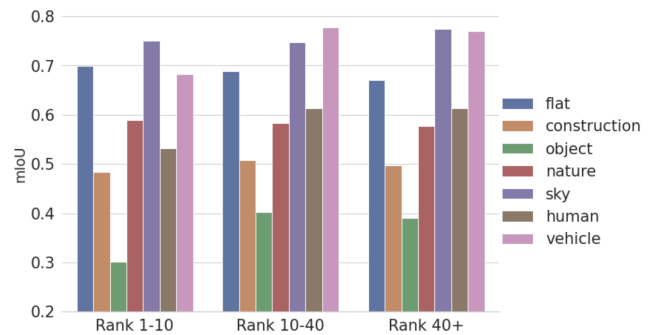


Figure 3. **CityScapes semantic segmentation model unfairness.** Class-level Intersection-over-Union (IoU) on the testing set differs significantly across the 3 city groups with different GDP attributes.

3.2. Datasets and sensitive groups

While several standard image datasets used in fairness studies exist, datasets with linked sensitive attribute information for real-world geographic imagery are very limited. We found three datasets which had or could be linked with attribute annotations for bias analyses. Next we describe sensitive group definitions for each dataset, based on location-based disparity context and attributes which could encode disproportionate spurious information, below.

LoveDA [61], urban or rural designation as sensitive attribute, is composed of 0.3m spatial resolution RGB satellite images collected from three cities in China. Images are annotated at pixel-level into 7 land-cover object classes, also with a label based on whether they are from an urban or rural district. Notably, images from the two groups have different class distributions. For example, urban areas contain more buildings and roads, while rural areas contain larger amounts of agriculture [61]. Moreover, it has been shown that model segmentation performances differ across urban and rural satellite images [73]. We split the original images into 512×512 pixel tiles, take 18% of the data for testing, and for the rest, 90% are for contrastive pre-training (5845 urban tiles and 5572 rural tiles) and 10% for fine-tuning.

EOLearn Slovenia [48], urban or rural designation as sensitive attribute, is composed of 10m spatial resolution Sentinel-2 images collected from whole region of Slovenia for the year 2017, with pixel-wise land cover annotations for 10 classes. We only use the RGB bands for the consistency with other datasets, remove images that have more than 10% of clouds, and split images into 256×256 pixel tiles to enlarge the training set. Labels are assigned by assessing if the center of each tile is located in urban boundaries or not (using urban municipality information¹ and administrative boundaries from OpenStreetMap²). This process generates 1760 urban tiles and 1996 rural tiles in total. Similar to the LoveDA process, 18% of the data are used for testing, and 90% of the rest of the data are used for pre-training and 10% for fine-tuning.

Cityscapes [6], GDP levels as sensitive attribute, is an urban street view dataset with pixel-level annotations available for 30 classes. The train and validation split from the original dataset are merged, then 18% of the data (900 images) are randomly selected for testing, and for the rest, 90% (3690 images) are used for pre-training and 10% (410 images) for fine-tuning. The group unfairness categories are identified by performing supervised training and evaluate on the testing images, where segmentation accuracy differences between cities are observed. In particular, we find that metropolitan cities tend to have worse accuracy than small cities. Therefore, we split the 21 cities into 3 groups by GDP level³, denoted as Rank 1-10, Rank 10-40 and Rank 40+, since GDP is a comprehensive factor related population density, infrastructure, and others that can affect street views. Group-level results are shown in Figure 3.

There are several major disparities visible. For instance, Rank 1-10 cities have lower accuracy on object, human, and vehicle, which could be because these classes exist in higher proportion in the images (statistics in Figure 10, Supplementary Material) and their positions commonly overlap, increasing segmentation difficulty. Slightly lower accuracy on the sky class for Rank 1-10 and Rank 10-40 cities may occur due to a higher prevalence of trees (nature class), traffic light and signs (object class) obstructing the sky and disturbing detection. In terms of overall accuracy, Rank 1-10 group has worst performance (IoU: 0.577) than the other two groups (0.613 for Rank 10-40 and 0.617 for Rank 40+).

3.3. Evaluation metrics

The quality of representations learnt from self-supervised pre-training is usually evaluated based on downstream task performance [20]. The principle behind this approach is using limited supervision and fine-tuning in assessment [13, 51, 71]. In line with this precedent, for com-

prehensively assessing representation quality, we report target task results every 1k iterations of fine-tuning for the pre-trained representation. On the downstream semantic segmentation task, we use Intersection-over-Union (IoU) as the accuracy metric, calculated using pixel-wise true positives (TP), false positives (FP), and false negatives (FN),

$$\text{IoU} := \frac{TP}{TP + FP + FN}.$$

Group accuracy for group g^i is computed via the mean of class-wise IoUs (referred to as μ_{g^i}).

We use two fairness metrics, both motivated by previous work in algorithmic fairness. First, the group difference with regard to accuracy [12, 39, 52, 77] (Diff). Diff for a 2-element sensitive attribute group $\{g^1, g^2\}$ is defined as:

$$\text{Diff} \{g^1, g^2\} := \frac{|\mu_{g^1} - \mu_{g^2}|}{\min\{\mu_{g^1}, \mu_{g^2}\}}.$$

And for $K \geq 3$ element group $\{g^1, \dots, g^K\}$, we measure group distances from parity [11]:

$$\text{Diff} \{g^1, \dots, g^K\} := \frac{K}{K-1} \sum_{i=1}^K \left| \frac{\mu_{g^i}}{\mu_{g^1} + \dots + \mu_{g^K}} - \frac{1}{K} \right|.$$

The second metric is worst group results (Wst), motivated by the problem of worsening overall performance for zero disparity [72]. Additionally, we define a fairness-accuracy trade-off criteria at optimal fine-tuning. We indicate that there is no trade-off (No TO) when fairness increases with no decrease in accuracy as compared to the vanilla baseline.

4. Methods

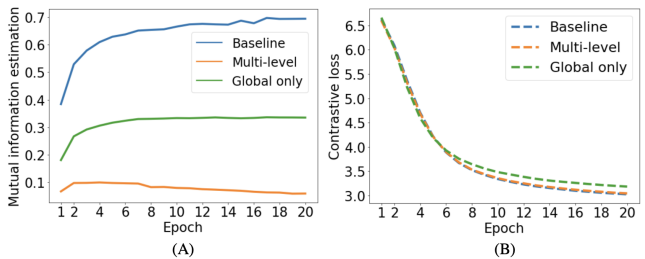


Figure 4. **Bias accumulation during contrastive pre-training.** (A) Sum of mutual information estimation, and (B) the contrastive loss of ResNet50 model with MoCo-V2 pre-training. The baseline method with no intervention (Baseline), regularizing only on the global feature vector (Global only), first two layers of feature maps (First-two only), last two layers of feature maps (Last-two only) all show bias residuals compared to the Multi-level method proposed as part of FairDCL.

4.1. Multi-level representation de-biasing

4.1.1 Backgrounds and definitions

The idea of constraining mutual information between representation and sensitive attribute to achieve fair learning

¹<https://www.gov.si/en/topics/towns-and-protected-areas-in-slovenia/>

²<https://www.openstreetmap.org/#map=12/40.7154/-74.1289>

³GDP level is measured by gross domestic product: https://en.wikipedia.org/wiki/List_of_German_cities_by_GDP

has multiple applications [22, 40, 76], which all operate on a global representation $\mathbf{z} = F(\mathbf{d})$, output from encoder F . However, fairness constraints only on the output layer do not guarantee that sensitive information is omitted from representation hierarchies of intermediate layers or blocks (herein we use the term “layer” for simplicity). As has been shown, the distribution of bias in terms of its category, number and strength is not constant across layers in contrastive self-supervised models [49]. Besides, layer-wise regularization is necessary to constrain the underlying representation space of CNN models [18, 19, 26]. We also validate this assumption empirically in Sec. 4.1.2. Local features in representation hierarchies are important [34, 63], especially when transferring to dense downstream tasks such as semantic segmentation, where representations are aggregated at different scales in order to let the decoder project predictions onto pixel space. Given the evidences in sum, we design a feature map based local mutual information estimation module and incorporate layer-wise fairness regularization into the contrastive optimization objective.

To measure mutual information $MI(X, S)$ between local feature X and the sensitive attribute $S = \{s_0, s_1, \dots\}$, we adapt the concat-and-convolve architecture in [16]. Notating the i^{th} layer as li , we first build a one-hot encoding map \mathbf{c}^{li} for sensitive attributes S whose size is same as the feature map \mathbf{x}^{li} output by li , and channel is the size of S . For each \mathbf{x}^{li} , a \mathbf{c}^{li} is built from the joint distribution of representation space X and attribute space S , and the marginal distribution of S separately, then the \mathbf{c}^{li} built in the two ways are concatenated with \mathbf{x}^{li} to form an “aligned” feature map pair, denoted as $P_{XS}(\mathbf{x}^{li} \parallel \mathbf{c}^{li})$, and a “shuffled” feature map pair, denoted as $P_{XP_S}(\mathbf{x}^{li} \parallel \mathbf{c}^{li})$. The mutual information between the aligned and shuffled feature map pairs will be estimated by a three-layer 1×1 convolutional discriminator D_i , using the JSD-derived formation [16]:

$$MI_{JSD}(X^{li}; S) := E_{P_{XS}}[-\text{sp}(-D_i(\mathbf{x}^{li} \parallel \mathbf{c}^{li}))] - E_{P_{XP_S}}[\text{sp}(D_i(\mathbf{x}^{li} \parallel \mathbf{c}^{li}))],$$

where $\text{sp}(a) = \log(1 + e^a)$, and D_i uses separate optimization to converge to the lower bound of MI_{JSD} .

4.1.2 Problem of residual sensitive information

We empirically validate the necessity to apply multi-level constraints to reduce bias accumulation across layers. We run self-supervised contrastive learning on LoveDA data using MoCo-v2 [5] with ResNet50 [14] as the base model. Simultaneous to model contrastive training, four independent discriminators are optimized to measure the mutual information $MI_{JSD}(\mathbf{x}^{li}; S)$ between representation output from the four residual layers and sensitive attribute urban/rural. MI_{JSD} are summed to measure the total amount of model bias for the data batch. Contrastive training is conducted for 7k iterations (around 20 epochs) and the mean bias of itera-

tions for each epoch is plotted in Figure 4 (A). The baseline training without MI_{JSD} constraints shows continually increasing and significantly higher bias than others. Adding a penalty loss which encourages minimizing MI_{JSD} only on the global representation or on subsets of layers both effectively control bias accumulation, however, their measurements are still high compared to intervening on all four layers (Multi-level), showing that global level regularization might remove partial bias but leave significant residual from earlier layers. The influence of this problem on model downstream performance will be tested with the method UnbiasedR (Sec. 5.2.1 and Table 1). The contrastive loss during training is plotted in Figure 4 (B), that all methods converge well; layer-wise mutual information constraints do not affect the contrastive learning objective. Both the debiasing and convergence benefits motivate us to learn fair multi-level representations for different encoder stages.

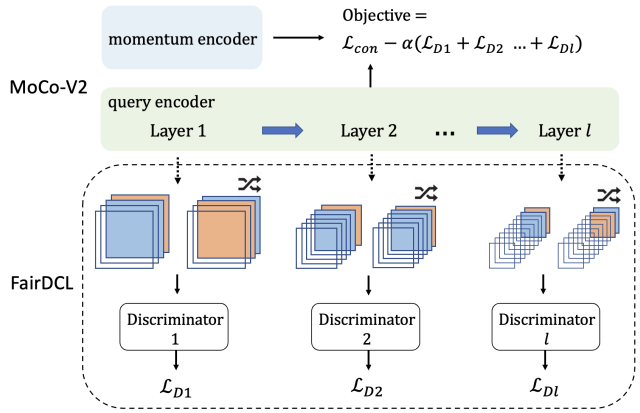


Figure 5. Overview of **FairDCL**, which captures sensitive information and applies fairness regularization on representation at multiple scales. We build one-hot feature maps to encode sensitive attribute and estimate mutual information by neural discriminators (details in Sec. 4.1.1). Penalty loss \mathcal{L}_{D_i} are computed accordingly and added into the final contrastive pre-training objective.

4.2. FairDCL pipeline

Figure 5 provides an overview of the proposed FairDCL method and the training process, with steps detailed in Algorithm 1. For each iteration of contrastive pre-training, learnt representation \mathbf{x}^{li} is yielded at layer li of the encoder F . Layer discriminators D_i are optimized by simultaneously estimating and maximizing MI_{JSD} with loss:

$$\mathcal{L}_{D_i}(\mathbf{x}^{li}, S; D_i) = -MI_{JSD}(\mathbf{x}^{li}; S). \quad (1)$$

Following [40], each discriminator is optimized for multiple inner rounds before encoder weights get updated. More rounds are desirable for discriminators to estimate mutual information with increased accuracy [40], and based on resource availability, we set a uniform round number $B = 20$. The architecture of D_i for each layer differs based on channel size of the concatenated feature map pair (implemented in Sec. 5.1). After discriminator optimization completes,

Algorithm 1: FairDCL. $F = \{l1, l2, ..li..., lN\}$ is the contrastive learning encoder. E is iterations per epoch; B is discriminators updating rounds; η is learning rate. α is fairness regularization strength.

for each iteration a from 1 to E **do**:
Encoder forward propagation:
 $\mathbf{x}^{lN}, \mathbf{x}^{lN-1}, \dots, \mathbf{x}^{l1} \leftarrow F(x)$ $\triangleright \mathbf{x}^{li}$ is the query representation output of the layer li
Discriminators updating:
for each round b from 1 to B **do**:
for each discriminator D_i **do**:
 $\mathcal{L}_{D_i} \leftarrow D_i(\mathbf{x}^{li} \parallel P_{XS}(\mathbf{c}^{li}), \mathbf{x}^{li} \parallel P_S(\mathbf{c}^{li}))$
 \triangleright Forward aligned and shuffled feature pairs
 $W_{D_i} \leftarrow W_{D_i} - \eta \nabla \mathcal{L}_{D_i}$ \triangleright Optimize D_i
Encoder updating:
 $\mathbf{x}^{lN}, \mathbf{x}^{lN-1}, \dots, \mathbf{x}^{l1}, q, k \leftarrow F(x)$ $\triangleright q, k$ is the query and key global representation
 $\mathcal{L}_{con} \leftarrow q, k$ \triangleright Compute contrastive loss
 $\mathcal{L}_D \leftarrow \sum_{i=1}^N \mathcal{L}_{D_i}$ \triangleright Compute MI loss
 $W_F \leftarrow W_F - \eta(\mathcal{L}_{con} - \alpha \mathcal{L}_D)$ \triangleright Update encoders

one iteration of encoder training is conducted wherein discriminators infer the multi-stage mutual information by loss in (1), and the losses are combined with the contrastive learning loss with a hyper-parameter α adjusting the fairness constraint strength. The final training objective is:

$$\mathcal{L}_F(X, S; D, F) = \mathcal{L}_{con} - \alpha \left(\sum_{li} \mathcal{L}_{D_i}(X^{li}, S; D_i) \right), \quad (2)$$

with which the encoder is encouraged to generate representation X with high \mathcal{L}_D , thus low MI_{JSD} . We apply FairDCL on the state-of-the-art contrastive learning framework MoCo-v2 [5]. The contrastive loss used for learning visual representation is InfoNCE [35], defined as:

$$\mathcal{L}_{con}(F) = -\log \frac{\exp(qk/\tau)}{\exp(qk/\tau) + \sum_j (q\hat{k}_j/\tau)}. \quad (3)$$

Here F consists of a query encoder and a key (or momentum) encoder, which outputs representation q and k from two augmented views of the same image, therefore k is viewed as ‘‘positive key’’. \hat{k}_j is a queue of representation encoded from different images in the dataset, viewed as ‘‘negative keys’’ [5]. \mathcal{L}_{con} encourages model to distinguish positive and negative keys so it can extract useful visual representation. The query encoder regularized by \mathcal{L}_D will be transferred to downstream tasks in fine-tuning.

Generalizability of FairDCL We note that our locality-sensitive de-biasing scheme applying intervention on embedding space can be integrated with any state-of-the-art convolution feature extractors, thus has the potential to be further promoted with different contrastive learning frameworks. Empirically, we experiment with the recently proposed DenseCL [63], which designs pixel-level positive and negative keys to better learn local feature correspondences.

Since the method fills the gap between pre-training and downstream dense prediction, it is suitable as an alternative contrastive learning framework for our proposed method.

5. Experiments

5.1. Implementation details

For contrastive pre-training: The base model of the encoders is ResNet50 [14], and mutual information discriminators D_i are built upon the query encoder (Figure 5), with 1×1 convolution layers (architecture details in Supplementary Material D). The contrastive pre-training runs for 10k iterations with a batch size of 32. Data augmentations used to generate positive and negative image view pairs are random greyscale conversion and random color jittering (no cropping, flips or rotations in order to retain local feature information). Hyper-parameter α , which scales the amount of mutual information loss \mathcal{L}_D in the total loss, is set to 0.5. Adam optimizer is used with a learning rate of 10^{-3} and weight decay of 10^{-4} for both encoders and discriminators. **Comparison methods** include state-of-the-art fair representation learning approaches: gradient reversal training (GR) by forcing encoders to generate representations that confuse a sensitive attribute classifier [39], domain independent training (DI) which samples data from same sensitive group in each training iteration to avoid leveraging sensitive domain boundaries [55, 65], and unbiased representation learning (UnbiasedR) [40] which uses mutual information to de-bias but operates only on a global space.

For semantic segmentation fine-tuning: We use UNet [43] with encoder weights transferred from the pre-training. The model is fine-tuned for 5k iterations with a batch size of 16 (around 76 epochs on LoveDA dataset, 284 epochs on Slovenia dataset, and 195 epochs on Cityscapes dataset). Since there lacks fine-tuning benchmark on used geographic datasets, we set the epoch numbers close to the fine-tuning settings in previous contrastive self-supervised learning studies [63, 74]. We evaluate metrics based on iterations rather than epochs to allow for direct computational comparison across datasets, following [24, 42]. We use cross-entropy (CE) loss as the training objective, and stochastic gradient descent (SGD) as the optimizer with a learning rate of 10^{-3} and a momentum of 0.9. The encoder part of the network is frozen during fine-tuning and no weight decay strategy is applied to avoid feature distortion [25]. Image augmentations used in the fine-tuning include random horizontal/vertical flips and random rotations.

5.2. Results

5.2.1 Downstream performances

Table 1 summarizes model fine-tuning results on semantic segmentation with the representation pre-trained with Baseline: vanilla MoCo-v2, and fairness-promoting methods:

Method	Iteration=1k			Iteration=2k			Iteration=3k			Iteration=4k			Iteration=5k			No TO	
	Diff(↓)	Wst(↑)	Acc(↑)														
LoveDA	Baseline	0.206	0.329	0.363	0.136	0.465	0.497	0.103	0.502	0.528	0.087	0.515	0.537	0.106	0.514	0.542	
	GR	0.176	0.358	0.390	0.113	0.450	0.474	0.070	0.502	0.519	0.088	0.496	0.517	0.089	0.517	0.540	✗
	DI	0.187	0.323	0.353	0.105	0.461	0.485	0.111	0.477	0.503	0.093	0.507	0.530	0.094	0.512	0.536	✗
	UnbiasedR	0.234	0.351	0.391	0.125	0.449	0.476	0.096	0.506	0.531	0.114	0.495	0.523	0.103	0.520	0.548	✓
	FairDCL	0.161	0.362	0.392	0.098	0.479	0.502	0.069	0.513	0.532	0.080	0.517	0.537	0.084	0.525	0.547	✓
Slovenia	Baseline	0.248	0.177	0.199	0.168	0.205	0.222	0.122	0.215	0.228	0.144	0.238	0.254	0.125	0.256	0.271	
	GR	0.231	0.180	0.200	0.134	0.202	0.216	0.119	0.231	0.244	0.146	0.231	0.249	0.134	0.253	0.268	✗
	DI	0.251	0.173	0.195	0.114	0.214	0.226	0.133	0.223	0.238	0.141	0.233	0.249	0.123	0.255	0.270	✗
	UnbiasedR	0.230	0.183	0.205	0.215	0.197	0.218	0.141	0.212	0.227	0.136	0.235	0.256	0.122	0.249	0.264	✗
	FairDCL	0.226	0.184	0.205	0.109	0.217	0.228	0.117	0.231	0.245	0.122	0.241	0.256	0.0801	0.262	0.273	✓
CityScapes	Baseline	0.0215	0.509	0.526	0.0253	0.530	0.551	0.0275	0.520	0.534	0.0248	0.541	0.560	0.0246	0.539	0.559	
	GR	0.0313	0.486	0.510	0.0298	0.487	0.509	0.0270	0.498	0.518	0.0255	0.510	0.530	0.0252	0.511	0.531	✗
	DI	0.0230	0.476	0.494	0.0229	0.506	0.524	0.0240	0.519	0.538	0.0251	0.523	0.543	0.0243	0.527	0.547	✗
	UnbiasedR	0.0208	0.493	0.508	0.0250	0.520	0.540	0.0237	0.518	0.535	0.0250	0.516	0.537	0.0245	0.518	0.537	✗
	FairDCL	0.0206	0.525	0.541	0.0238	0.536	0.546	0.0236	0.537	0.557	0.0248	0.545	0.566	0.0241	0.545	0.564	✓

Table 1. **Downstream semantic segmentation results** on LoveDA, Slovenia, CityScapes dataset for 5k fine-tuning iterations. The encoder weights are learnt with 5 comparison pre-training methods. Our FairDCL shows clear improvements on fairness metrics (Diff and Wst) and accuracy metric (Acc) over baseline and prior methods throughout the training, also we do not see a fairness-accuracy trade-off (No TO) on all datasets. Results are the mean over 5 independent runs, and the standard deviations are provided in the Supplementary Material.

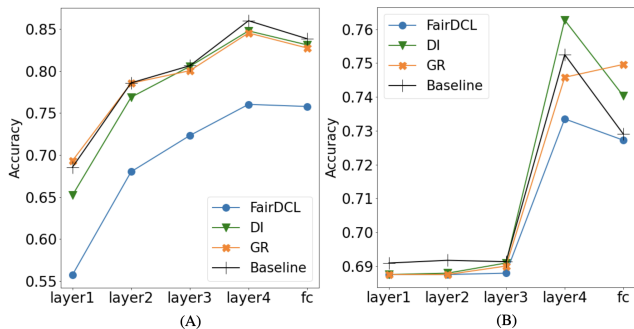


Figure 6. **Linear separation evaluation:** We train a linear layer on top of each representation level, including feature maps of intermediate residual layers and the global feature (“fc”), to classify sensitive attributes: urban/rural on (A) LoveDA, and female/male on (B) MS-COCO. Lower accuracy is good: it indicates harder to predict sensitive attributes using the pre-trained representation.

GR, DI, UnbiasedR, and FairDCL, on the three geographic image datasets: LoveDA, Slovenia, and CityScapes. Segmentation accuracy and fairness metrics are reported every 1k iterations and we include results from 1k to 5k iterations to compare representation quality in term of its influence on the whole fine-tuning procedure (extended iterations are shown in the ablation study). “No TO” indicates if a method waives the fairness-accuracy trade-off problem, that in its best fine-tuning round, whether the improved “Diff” metric does **not** cause a worse “Acc” metric. Such trade-off robustness with respect to the other fairness metric “Wst” is depicted in Figure 13 in the Supplementary Material E.

We first note that across iterations, FairDCL nearly always outperforms other approaches in terms of fairness. FairDCL obtains the smallest cross-group difference (Diff) and highest worst group result (Wst), indicating that the rep-

resentations trained with multi-scale fairness constrains can lead to higher group parity meanwhile maximizing performance of the worst case groups (urban or rural places in LoveDA and Slovenia, or cities with different GDP levels in CityScapes). Results also show the stability of the learnt representations, that the downstream training shifts, such as fine-tuning the decoder for shorter or longer rounds, do not break model advantages achieved by FairDCL.

Importantly, FairDCL is the only method that does not show a fairness-accuracy trade-off on all three datasets. FairDCL in general obtains comparable or better overall accuracy to Baseline, demonstrating robust model quality in addition to fairness. In contrast, GR and DI show lower overall accuracy, especially on the CityScapes dataset. This observation resonates with the intrinsic trade-off problem pointed out by previous fairness studies [17, 72, 72, 77]; DI allows building image contrastive pairs only from a fraction of data which can discount model learning [65], while the adversarial approach used in GR can be counter-productive if the adversary is not trained enough to achieve the infimum [33], which could all potentially degrade model quality for group equalization. Our adapted mutual information discriminators use information-theoretic objectives, which are shown to be optimized without competing with the encoder so can match or exceed state-of-the-art adversarial debiasing methods [33, 40]. FairDCL further illustrates that applying the mutual information constraints on multiple encoder outputs can better extend fairness to pixel-level applications. In contrast, UnbiasedR, the counterpart method which applies constraints at the single image level, shows no trade-off on LoveDA dataset, and has worse results on both fairness metrics than FairDCL (Table 1).

Using the alternative self-supervised contrastive learning

framework DenseCL, similar advantages can be observed, the fairness improvement with no trade-off of FairDCL pre-trained feature encoder for the downstream segmentation predictions (Table 10 in the Supplementary Material E).

5.2.2 Embedding spaces

To further trace how FairDCL improves fairness, we analyze a linear separation property [42] on embedding spaces to assess how well a linear model can differentiate sensitive attributes using learnt representations. High separation degree indicates the embedding space and attribute are differentiable [4, 35, 42], which could be used in prediction and cause bias, thus is not desirable here. We freeze the trained ResNet50 encoder and use a fully connected layer on top of representation output from different layers for sensitive attribute label classification. Figure 6 (A) presents the classification score on urban/rural attribute on LoveDA: FairDCL obtains the lowest attribute differentiation results for all embedding stages and global stage of representation, indicating that the encoder trained with FairDCL has favorably learnt the least sensitive information at pixel-level features during the contrastive pre-training.

Though we focus on geographic images, we check the method’s generalizability to a different image domain by conducting contrastive pre-training on MS-COCO [27], a dataset commonly used in fairness studies [53, 60, 62]. Sensitive attribute gender, categorized as “female” or “male”, is obtained from [75]. There are 2901 images with female and 6567 images with male labels. Linear analysis results show that FairDCL again produces the desired lowest classification accuracies (Figure 6 (B)), but unlike in Figure 6 (A), it does not surpass the comparison methods much. This is likely because while geographic attributes are represented at a pixel-level, human faces/objects may not be represented through local features, thus gender attributes are less pronounced as pixel-level biases in dense representation learning, which is what our proposed approach focuses on.

Method	Iteration=6k			Iteration=7k			Iteration=8k			No TO
	Diff(↓)	Wst (↑)	Acc(↑)	Diff	Wst	Acc	Diff	Wst	Acc	
Baseline	0.106	0.533	0.566	0.109	0.529	0.558	0.097	0.536	0.562	
GR	0.092	0.538	0.563	0.093	0.535	0.559	0.094	0.538	0.560	✗
DI	0.087	0.537	0.561	0.090	0.533	0.557	0.084	0.530	0.552	✗
UnbiasedR	0.109	0.538	0.567	0.114	0.542	0.570	0.123	0.534	0.567	✗
FairDCL	0.089	0.543	0.567	0.82	0.542	0.564	0.73	0.549	0.569	✓

Table 2. **Ablation study for downstream training shifts** on LoveDA dataset for 5k-8k iterations. Our FairDCL method maintains the advantage in fairness improvements (Diff and Wst) over Baseline without a trade-off of mean accuracy (Acc).

5.2.3 Ablation studies

Training schedules. We run longer training on the labeled downstream data to validate fine-tuning stability of the pre-

$\alpha = 0.1$			$\alpha = 0.5$			$\alpha = 1$			$\alpha = 10$		
Diff(↓)	Wst (↑)	Acc(↑)	Diff	Wst	Acc	Diff	Wst	Acc	Diff	Wst	Acc
0.096	0.519	0.544	0.084	0.525	0.547	0.075	0.521	0.540	0.069	0.521	0.539

Table 3. **Ablation study for discriminator weights.** The best fine-tuning results are shown for the encoder pre-trained with different weight, $\alpha = 0.1, 0.5, 1, 10$, of the proposed objective.

Method	Urban:68% Rural:32%				Urban:35% Rural:65%			
	Diff(↓)	Wst (↑)	Acc(↑)	No TO	Diff(↓)	Wst (↑)	Acc(↑)	No TO
Baseline	0.214	0.337	0.373		0.253	0.341	0.384	
GR	0.209	0.329	0.364	✗	0.218	0.350	0.387	✓
DI	0.203	0.332	0.364	✗	0.206	0.330	0.364	✗
UnbiasedR	0.166	0.363	0.393	✓	0.229	0.338	0.377	✗
FairDCL	0.123	0.394	0.418	✓	0.198	0.352	0.388	✓

Table 4. **Ablation study for unbalanced data distribution** The proportion of sensitive groups in the pre-training data is adjusted such that one group has much less representation. FairDCL performs consistently with data balance changes.

trained encoders. Shown in Table 2, in general, all methods converge and reach performance plateau after 6k iterations. The converged results should be bounded by the capacity of the decoder component, so we only show results until 8k iterations. Results give further evidence that the benefits of the de-biased representations pre-trained with FairDCL do not vanish in longer training regimes.

Discriminator weights. An ablation study for hyper-parameter α which scales discriminator loss \mathcal{L}_D , thus the fairness regularization strength in FairDCL is shown in Table 3. The method is overall robust to the parameter; a large weight like 10 will not completely corrupt the downstream accuracy. Using smaller α have higher Wst, while larger α have higher Diff, and we select $\alpha = 0.5$ for a balance.

Data distribution. The sensitive attribute urban and rural have comparable training samples in earlier experiments (LoveDA is 5.8k and 5.5k, EOlearn Slovenia is 1.7k and 1.9k for urban/rural, but Cityscapes is highly unbalanced: 1.8k, 0.78k, 1.1k for the three GDP groups). Here we intentionally remove part of pre-training samples for certain groups to create more unbalanced subsets. With performances shown in Table 4, our method shows robustness under the two less even attribute distributions.

6. Conclusions

In this work, we identify and address unique fairness challenges in semantic segmentation of geographic images such as satellite images and street view images. We theoretically define the scenario with a causal graph, showing that contrastive self-supervised pre-training can utilize spurious land-cover object features and accumulate sensitive attribute-correlated bias, resulting in disparate downstream segmentation accuracy. Then we address it by a mutual

information training objective to learn good local features with minimal spurious representations. Experimental results show fairer segmentation results pre-trained with the method on multiple geographic datasets and different sensitive groups. In addition to performance gain, the method consistently avoids the trade-off between fairness and accuracy. As future directions, first, more geographic domains can be explored and the fairness analysis can be scaled to greater number of attributes. Second, sensitive attribute encoding besides one-hot feature map can be explored. We encourage experimenting with different encoding mechanisms and mutual information estimators to improve performance across different real-world settings.

References

- [1] Kumar Ayush, Burak Uzkent, Chenlin Meng, Kumar Tanmay, Marshall Burke, David Lobell, and Stefano Ermon. Geography-aware self-supervised learning. In *Proceedings of the IEEE/CVF International Conference on Computer Vision*, pages 10181–10190, 2021. 1, 2
- [2] Mohamed Ishmael Belghazi, Aristide Baratin, Sai Rajeshwar, Sherjil Ozair, Yoshua Bengio, Aaron Courville, and Devon Hjelm. Mutual information neural estimation. In *International conference on machine learning*, pages 531–540. PMLR, 2018. 2
- [3] Krishna Chaitanya, Ertunc Erdil, Neerav Karani, and Ender Konukoglu. Contrastive learning of global and local features for medical image segmentation with limited annotations. *Advances in Neural Information Processing Systems*, 33:12546–12558, 2020. 2
- [4] Ting Chen, Simon Kornblith, Mohammad Norouzi, and Geoffrey Hinton. A simple framework for contrastive learning of visual representations. In *International conference on machine learning*, pages 1597–1607. PMLR, 2020. 2, 8
- [5] Xinlei Chen, Haoqi Fan, Ross Girshick, and Kaiming He. Improved baselines with momentum contrastive learning. *arXiv preprint arXiv:2003.04297*, 2020. 2, 5, 6
- [6] Marius Cordts, Mohamed Omran, Sebastian Ramos, Timo Rehfeld, Markus Enzweiler, Rodrigo Benenson, Uwe Franke, Stefan Roth, and Bernt Schiele. The cityscapes dataset for semantic urban scene understanding. In *Proceedings of the IEEE conference on computer vision and pattern recognition*, pages 3213–3223, 2016. 4
- [7] Elliot Creager, David Madras, Jörn-Henrik Jacobsen, Marissa Weis, Kevin Swersky, Toniann Pitassi, and Richard Zemel. Flexibly fair representation learning by disentanglement. In *International conference on machine learning*, pages 1436–1445. PMLR, 2019. 2
- [8] Terrance de Vries, Ishan Misra, Changhan Wang, and Laurens van der Maaten. Does object recognition work for everyone? In *Proceedings of the IEEE/CVF Conference on Computer Vision and Pattern Recognition (CVPR) Workshops*, June 2019. 1
- [9] Ranjith Dinakaran, Li Zhang, Chang-Tsun Li, Ahmed Bouridane, and Richard Jiang. Robust and fair undersea target detection with automated underwater vehicles for biodiversity data collection. *Remote Sensing*, 14(15):3680, 2022. 2
- [10] Linus Ericsson, Henry Gouk, and Timothy M Hospedales. How well do self-supervised models transfer? In *Proceedings of the IEEE/CVF Conference on Computer Vision and Pattern Recognition*, pages 5414–5423, 2021. 1
- [11] Rina Friedberg, Stuart Ambler, and Guillaume Saint-Jacques. Representation-aware experimentation: Group inequality analysis for a/b testing and alerting. *arXiv preprint arXiv:2204.12011*, 2022. 4
- [12] Sixue Gong, Xiaoming Liu, and Anil K Jain. Mitigating face recognition bias via group adaptive classifier. In *Proceedings of the IEEE/CVF conference on computer vision and pattern recognition*, pages 3414–3424, 2021. 4
- [13] Priya Goyal, Dhruv Mahajan, Abhinav Gupta, and Ishan Misra. Scaling and benchmarking self-supervised visual representation learning. In *Proceedings of the IEEE/CVF International Conference on computer vision*, pages 6391–6400, 2019. 4
- [14] Kaiming He, Xiangyu Zhang, Shaoqing Ren, and Jian Sun. Deep residual learning for image recognition. In *Proceedings of the IEEE conference on computer vision and pattern recognition*, pages 770–778, 2016. 5, 6
- [15] Dan Hendrycks, Mantas Mazeika, Saurav Kadavath, and Dawn Song. Using self-supervised learning can improve model robustness and uncertainty. *Advances in neural information processing systems*, 32, 2019. 2
- [16] R Devon Hjelm, Alex Fedorov, Samuel Lavoie-Marchildon, Karan Grewal, Phil Bachman, Adam Trischler, and Yoshua Bengio. Learning deep representations by mutual information estimation and maximization. *arXiv preprint arXiv:1808.06670*, 2018. 2, 5
- [17] Lily Hu and Yiling Chen. Fair classification and social welfare. In *Proceedings of the 2020 Conference on Fairness, Accountability, and Transparency*, pages 535–545, 2020. 7
- [18] Zhuolin Jiang, Yaming Wang, Larry Davis, Walter Andrews, and Viktor Rozgic. Learning discriminative features via label consistent neural network. In *2017 IEEE Winter Conference on Applications of Computer Vision (WACV)*, pages 207–216. IEEE, 2017. 5
- [19] Xiaojie Jin, Yunpeng Chen, Jian Dong, Jiashi Feng, and Shuicheng Yan. Collaborative layer-wise discriminative learning in deep neural networks. In *European Conference on Computer Vision*, pages 733–749. Springer, 2016. 5
- [20] Longlong Jing and Yingli Tian. Self-supervised visual feature learning with deep neural networks: A survey. *IEEE transactions on pattern analysis and machine intelligence*, 43(11):4037–4058, 2020. 4
- [21] Sangwon Jung, Donggyu Lee, Taeon Park, and Taesup Moon. Fair feature distillation for visual recognition. In *Proceedings of the IEEE/CVF conference on computer vision and pattern recognition*, pages 12115–12124, 2021. 1

- [22] Byungju Kim, Hyunwoo Kim, Kyungsu Kim, Sungjin Kim, and Junmo Kim. Learning not to learn: Training deep neural networks with biased data. In *Proceedings of the IEEE/CVF Conference on Computer Vision and Pattern Recognition*, pages 9012–9020, 2019. 5
- [23] Justin B Kinney and Gurinder S Atwal. Equitability, mutual information, and the maximal information coefficient. *Proceedings of the National Academy of Sciences*, 111(9):3354–3359, 2014. 2
- [24] Simon Kornblith, Jonathon Shlens, and Quoc V Le. Do better imagenet models transfer better? In *Proceedings of the IEEE/CVF conference on computer vision and pattern recognition*, pages 2661–2671, 2019. 6
- [25] Ananya Kumar, Aditi Raghunathan, Robbie Jones, Tengyu Ma, and Percy Liang. Fine-tuning can distort pretrained features and underperform out-of-distribution. *arXiv preprint arXiv:2202.10054*, 2022. 6
- [26] Zhe Li, Wieland Brendel, Edgar Walker, Erick Cobos, Taliah Muhammad, Jacob Reimer, Matthias Bethge, Fabian Sinz, Zachary Pitkow, and Andreas Tolias. Learning from brains how to regularize machines. *Advances in neural information processing systems*, 32, 2019. 5
- [27] Tsung-Yi Lin, Michael Maire, Serge Belongie, James Hays, Pietro Perona, Deva Ramanan, Piotr Dollár, and C Lawrence Zitnick. Microsoft coco: Common objects in context. In *European conference on computer vision*, pages 740–755. Springer, 2014. 8
- [28] Subhabrata Majumdar, Cheryl Flynn, and Ritwik Mitra. Detecting bias in the presence of spatial autocorrelation. In *Algorithmic Fairness through the Lens of Causality and Robustness workshop*, pages 6–18. PMLR, 2022. 1
- [29] Ninareh Mehrabi, Fred Morstatter, Nripsuta Saxena, Kristina Lerman, and Aram Galstyan. A survey on bias and fairness in machine learning. *ACM Computing Surveys (CSUR)*, 54(6):1–35, 2021. 1
- [30] Vishwali Mhasawade, Yuan Zhao, and Rumi Chunara. Machine learning and algorithmic fairness in public and population health. *Nature Machine Intelligence*, 3(8):659–666, 2021. 1
- [31] Ishan Misra and Laurens van der Maaten. Self-supervised learning of pretext-invariant representations. In *Proceedings of the IEEE/CVF Conference on Computer Vision and Pattern Recognition*, pages 6707–6717, 2020. 2
- [32] Aythami Morales, Julian Fierrez, Ruben Vera-Rodriguez, and Ruben Tolosana. Sensitenets: Learning agnostic representations with application to face images. *IEEE Transactions on Pattern Analysis and Machine Intelligence*, 43(6):2158–2164, 2020. 2
- [33] Daniel Moyer, Shuyang Gao, Rob Brekelmans, Aram Galstyan, and Greg Ver Steeg. Invariant representations without adversarial training. *Advances in Neural Information Processing Systems*, 31, 2018. 7
- [34] Pedro O O Pinheiro, Amjad Almahairi, Ryan Benmalek, Florian Golemo, and Aaron C Courville. Unsupervised learning of dense visual representations. *Advances in Neural Information Processing Systems*, 33:4489–4500, 2020. 2, 5
- [35] Aaron van den Oord, Yazhe Li, and Oriol Vinyals. Representation learning with contrastive predictive coding. *arXiv preprint arXiv:1807.03748*, 2018. 6, 8
- [36] Sungho Park, Sunhee Hwang, Dohyung Kim, and Hyeran Byun. Learning disentangled representation for fair facial attribute classification via fairness-aware information alignment. In *Proceedings of the AAAI Conference on Artificial Intelligence*, volume 35, pages 2403–2411, 2021. 2
- [37] Sungho Park, Jewook Lee, Pilhyeon Lee, Sunhee Hwang, Dohyung Kim, and Hyeran Byun. Fair contrastive learning for facial attribute classification. In *Proceedings of the IEEE/CVF Conference on Computer Vision and Pattern Recognition*, pages 10389–10398, 2022. 2
- [38] Esther Puyol-Antón, Bram Ruijsink, Stefan K Piechnik, Stefan Neubauer, Steffen E Petersen, Reza Razavi, and Andrew P King. Fairness in cardiac mr image analysis: an investigation of bias due to data imbalance in deep learning based segmentation. In *International Conference on Medical Image Computing and Computer-Assisted Intervention*, pages 413–423. Springer, 2021. 2
- [39] Edward Raff and Jared Sylvester. Gradient reversal against discrimination: A fair neural network learning approach. In *2018 IEEE 5th International Conference on Data Science and Advanced Analytics (DSAA)*, pages 189–198. IEEE, 2018. 2, 4, 6
- [40] Ruggero Ragonesi, Riccardo Volpi, Jacopo Cavazza, and Vittorio Murino. Learning unbiased representations via mutual information backpropagation. In *Proceedings of the IEEE/CVF Conference on Computer Vision and Pattern Recognition*, pages 2729–2738, 2021. 2, 5, 6, 7
- [41] Vikram V Ramaswamy, Sunnie SY Kim, and Olga Russakovsky. Fair attribute classification through latent space de-biasing. In *Proceedings of the IEEE/CVF conference on computer vision and pattern recognition*, pages 9301–9310, 2021. 1, 2
- [42] Colorado J Reed, Xiangyu Yue, Ani Nrusimha, Sayna Ebrahimi, Vivek Vijaykumar, Richard Mao, Bo Li, Shanghang Zhang, Devin Guillory, Sean Metzger, et al. Self-supervised pretraining improves self-supervised pretraining. In *Proceedings of the IEEE/CVF Winter Conference on Applications of Computer Vision*, pages 2584–2594, 2022. 2, 6, 8
- [43] Olaf Ronneberger, Philipp Fischer, and Thomas Brox. U-net: Convolutional networks for biomedical image segmentation. In *International Conference on Medical image computing and computer-assisted intervention*, pages 234–241. Springer, 2015. 6
- [44] Sudipan Saha, Lichao Mou, Chunping Qiu, Xiao Xiang Zhu, Francesca Bovolo, and Lorenzo Bruzzone. Unsupervised deep joint segmentation of multitemporal high-resolution images. *IEEE Transactions on Geoscience and Remote Sensing*, 58(12):8780–8792, 2020. 1

- [45] Linus Scheibenreif, Joëlle Hanna, Michael Mommert, and Damian Borth. Self-supervised vision transformers for land-cover segmentation and classification. In *Proceedings of the IEEE/CVF Conference on Computer Vision and Pattern Recognition*, pages 1422–1431, 2022. 1
- [46] Ignacio Serna, Aythami Morales, Julian Fierrez, and Nick Obradovich. Sensitive loss: Improving accuracy and fairness of face representations with discrimination-aware deep learning. *Artificial Intelligence*, 305:103682, 2022. 2
- [47] MAS Setianto and A Gamal. Spatial justice in the distribution of public services. In *IOP Conference Series: Earth and Environmental Science*, volume 673, page 012024. IOP Publishing, 2021. 1
- [48] Sinergise. Modified copernicus sentinel data 2017/sentinel hub. <https://sentinel-hub.com/>, 2022. 4
- [49] Kirill Sirotkin, Pablo Carballeira, and Marcos Escudero-Viñolo. A study on the distribution of social biases in self-supervised learning visual models. In *Proceedings of the IEEE/CVF Conference on Computer Vision and Pattern Recognition*, pages 10442–10451, 2022. 2, 5
- [50] Robert Soden, Dennis Wagenaar, Dave Luo, and Annetien Tijssen. Taking ethics, fairness, and bias seriously in machine learning for disaster risk management. *arXiv preprint arXiv:1912.05538*, 2019. 1
- [51] Jong-Chyi Su, Subhransu Maji, and Bharath Hariharan. When does self-supervision improve few-shot learning? In *European conference on computer vision*, pages 645–666. Springer, 2020. 4
- [52] Attila Szabó, Hadi Jamali-Rad, and Siva-Datta Mannava. Tilted cross-entropy (tce): Promoting fairness in semantic segmentation. In *Proceedings of the IEEE/CVF Conference on Computer Vision and Pattern Recognition*, pages 2305–2310, 2021. 2, 4
- [53] Ruixiang Tang, Mengnan Du, Yuening Li, Zirui Liu, Na Zou, and Xia Hu. Mitigating gender bias in captioning systems. In *Proceedings of the Web Conference 2021*, pages 633–645, 2021. 8
- [54] Huan Tian, Tianqing Zhu, Wei Liu, and Wanlei Zhou. Image fairness in deep learning: problems, models, and challenges. *Neural Computing and Applications*, pages 1–19, 2022. 1
- [55] Yao-Hung Hubert Tsai, Martin Q Ma, Han Zhao, Kun Zhang, Louis-Philippe Morency, and Ruslan Salakhutdinov. Conditional contrastive learning: Removing undesirable information in self-supervised representations. *arXiv preprint arXiv:2106.02866*, 2021. 2, 6
- [56] Yao-Hung Hubert Tsai, Yue Wu, Ruslan Salakhutdinov, and Louis-Philippe Morency. Self-supervised learning from a multi-view perspective. *arXiv preprint arXiv:2006.05576*, 2020.
- [57] Michael Tschannen, Josip Djolonga, Paul K Rubenstein, Sylvain Gelly, and Mario Lucic. On mutual information maximization for representation learning. *arXiv preprint arXiv:1907.13625*, 2019.
- [58] Wouter Van Gansbeke, Simon Vandenhende, Stamatios Georgoulis, and Luc V Gool. Revisiting contrastive methods for unsupervised learning of visual representations. *Advances in Neural Information Processing Systems*, 34:16238–16250, 2021. 1
- [59] Yen Nhi Truong Vu, Richard Wang, Niranjan Balachandar, Can Liu, Andrew Y Ng, and Pranav Rajpurkar. Medaug: Contrastive learning leveraging patient metadata improves representations for chest x-ray interpretation. In *Machine Learning for Healthcare Conference*, pages 755–769. PMLR, 2021. 2
- [60] Jialu Wang, Yang Liu, and Xin Eric Wang. Are gender-neutral queries really gender-neutral? mitigating gender bias in image search. *arXiv preprint arXiv:2109.05433*, 2021. 8
- [61] Junjue Wang, Zhuo Zheng, Ailong Ma, Xiaoyan Lu, and Yanfei Zhong. Loveda: A remote sensing land-cover dataset for domain adaptive semantic segmentation. *arXiv preprint arXiv:2110.08733*, 2021. 3
- [62] Tianlu Wang, Jieyu Zhao, Mark Yatskar, Kai-Wei Chang, and Vicente Ordonez. Balanced datasets are not enough: Estimating and mitigating gender bias in deep image representations. In *Proceedings of the IEEE/CVF International Conference on Computer Vision*, pages 5310–5319, 2019. 1, 8
- [63] Xinlong Wang, Rufeng Zhang, Chunhua Shen, Tao Kong, and Lei Li. Dense contrastive learning for self-supervised visual pre-training. In *Proceedings of the IEEE/CVF Conference on Computer Vision and Pattern Recognition*, pages 3024–3033, 2021. 2, 5, 6, 14
- [64] Yi Wang, Conrad M Albrecht, Nassim Ait Ali Braham, Lichao Mou, and Xiao Xiang Zhu. Self-supervised learning in remote sensing: A review. *arXiv preprint arXiv:2206.13188*, 2022. 1
- [65] Zeyu Wang, Klint Qinami, Ioannis Christos Karakozis, Kyle Genova, Prem Nair, Kenji Hata, and Olga Russakovsky. Towards fairness in visual recognition: Effective strategies for bias mitigation. In *Proceedings of the IEEE/CVF conference on computer vision and pattern recognition*, pages 8919–8928, 2020. 6, 7
- [66] Zhirong Wu, Yuanjun Xiong, Stella X Yu, and Dahua Lin. Unsupervised feature learning via non-parametric instance discrimination. In *Proceedings of the IEEE conference on computer vision and pattern recognition*, pages 3733–3742, 2018. 2
- [67] Zhenda Xie, Yutong Lin, Zheng Zhang, Yue Cao, Stephen Lin, and Han Hu. Propagate yourself: Exploring pixel-level consistency for unsupervised visual representation learning. In *Proceedings of the IEEE/CVF Conference on Computer Vision and Pattern Recognition*, pages 16684–16693, 2021. 2
- [68] Yuwen Xiong, Mengye Ren, and Raquel Urtasun. Loco: Local contrastive representation learning. *Advances in neural information processing systems*, 33:11142–11153, 2020. 2
- [69] Xingkun Xu, Yuge Huang, Pengcheng Shen, Shaoxin Li, Jilin Li, Feiyue Huang, Yong Li, and Zhen Cui. Consistent

instance false positive improves fairness in face recognition. In *Proceedings of the IEEE/CVF conference on computer vision and pattern recognition*, pages 578–586, 2021. [2](#)

- [70] Haolin Yuan, Armin Hadzic, William Paul, Daniella Villegas de Flores, Philip Mathew, John Aucott, Yinzhi Cao, and Philippe Burlina. Edgemixup: Improving fairness for skin disease classification and segmentation. *arXiv preprint arXiv:2202.13883*, 2022. [2](#)
- [71] Xiaohua Zhai, Joan Puigcerver, Alexander Kolesnikov, Pierre Ruysen, Carlos Riquelme, Mario Lucic, Josip Djolonga, Andre Susano Pinto, Maxim Neumann, Alexey Dosovitskiy, et al. A large-scale study of representation learning with the visual task adaptation benchmark. *arXiv preprint arXiv:1910.04867*, 2019. [4](#)
- [72] Haoran Zhang, Natalie Dullerud, Karsten Roth, Lauren Oakden-Rayner, Stephen Pfohl, and Marzyeh Ghassemi. Improving the fairness of chest x-ray classifiers. In *Conference on Health, Inference, and Learning*, pages 204–233. PMLR, 2022. [4](#), [7](#)
- [73] Miao Zhang, Harvineet Singh, Lazarus Chok, and Rumi Chunara. Segmenting across places: The need for fair transfer learning with satellite imagery. In *Proceedings of the IEEE/CVF Conference on Computer Vision and Pattern Recognition*, pages 2916–2925, 2022. [1](#), [3](#)
- [74] Yifan Zhang, Bryan Hooi, Dapeng Hu, Jian Liang, and Jiashi Feng. Unleashing the power of contrastive self-supervised visual models via contrast-regularized fine-tuning. *Advances in Neural Information Processing Systems*, 34:29848–29860, 2021. [6](#)
- [75] Dora Zhao, Angelina Wang, and Olga Russakovsky. Understanding and evaluating racial biases in image captioning. In *Proceedings of the IEEE/CVF International Conference on Computer Vision*, pages 14830–14840, 2021. [8](#)
- [76] Wei Zhu, Haitian Zheng, Haofu Liao, Weijian Li, and Jiebo Luo. Learning bias-invariant representation by cross-sample mutual information minimization. In *Proceedings of the IEEE/CVF International Conference on Computer Vision*, pages 15002–15012, 2021. [2](#), [5](#)
- [77] Dominik Zietlow, Michael Lohaus, Guha Balakrishnan, Matthäus Kleindessner, Francesco Locatello, Bernhard Schölkopf, and Chris Russell. Leveling down in computer vision: Pareto inefficiencies in fair deep classifiers. In *Proceedings of the IEEE/CVF Conference on Computer Vision and Pattern Recognition*, pages 10410–10421, 2022. [4](#), [7](#), [14](#)

Supplementary Material: Fair contrastive pre-training for geographic images

A. Examples of unfairness in land-cover object semantic segmentation

Besides segmentation disparities for different “road” variations shown in Figure 1, here we provide examples for “building”, “water”, and “forest” classes, and their corresponding spurious and robust features in Figure 7, Figure 8, and Figure 9. In each caption, based on simple visual assessment, we provide examples of possible aspects of the images that could contribute to spurious or robust features.

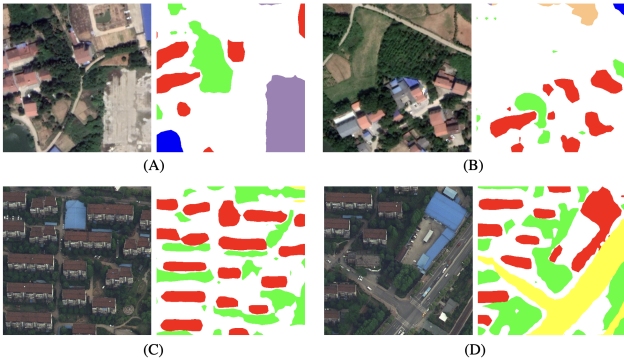


Figure 7. **Segmentation bias for “building” class.** Compared to the scattered rural buildings in (A) and (B), urban buildings that have uniform shapes and neat arrangements are better segmented (C) and (D), and especially have their edges detected more precisely. Spurious features of building objects could include the shapes, e.g. rectangular or irregular shapes, and/or the colors. Robust aspects of buildings can include the shape of their clustering and/or height in relation to surroundings.

B. Class distribution shifts across groups

Class distributions also vary across sensitive groups; we plot class distributions in terms of proportion of pixels per class by group for each of the three datasets, in Figure 10, Figure 11, and Figure 12.

C. Mutual information discriminators

The base model used as the encoder in our experiments is ResNet50. Multi-stage mutual information discriminators are built for representation outputs of four layers (residual blocks). In Table 5 to Table 8 we provide the architecture dimensions for each discriminator and the input and output feature map channel sizes C , noting that feature map height H and width W vary across datasets, depending on the size of images the model is trained on.

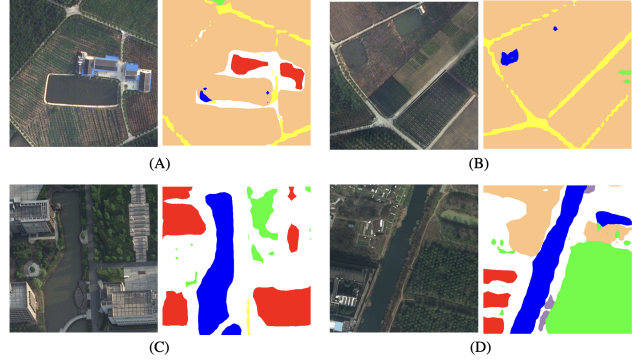


Figure 8. **Segmentation bias for “water” class.** The model has difficulty distinguishing water from agriculture land, especially when the water area is small as in (A) and (B). In comparison, water that is surrounded by more different landscapes are much better segmented as in (C) and (D). Spurious features of water object could include the shape and color: rural areas have more small water ponds, and the water colors can vary potentially based on depth of the water source. Robust features could include the texture of the water surface which is generally more smooth compared to other land-covers.

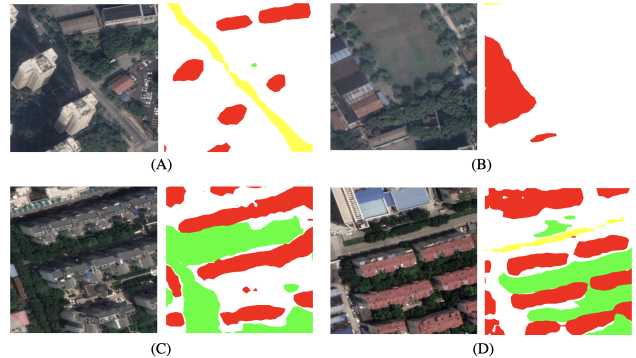


Figure 9. **Segmentation bias for “forest” class.** Forests/trees that are in open areas are largely neglected by the model in (A) and (B), while in contrast, trees in between building blocks are well detected as in (C) and (D). The development of urban greening promotes growing trees along streets or buildings, which could be a spurious feature for model to use, that the feature does not generalize to trees grown in open fields, a common case rural area. A more robust feature of trees should be texture of tree crowns that is generalizable and distinguishable.

Layer	Input	Output
1×1 Conv2D (258, 258)	258	258
1×1 Conv2D (258, 20)	258	20
1×1 Conv2D (20, 1)	20	1

Table 5. Discriminator for layer1 of ResNet50 encoder.

The outputs of each discriminator are a $H \times W$ matrix for the “shuffled” feature map pair and the “aligned” fea-

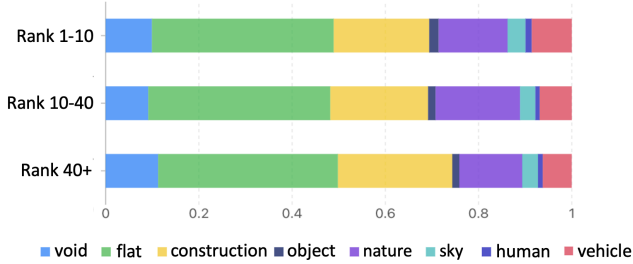


Figure 10. **CityScapes dataset class distribution shifts:** Class distribution for images from the three groups: Rank 1-10, Rank 10-40, and Rank 40+ of the CityScapes dataset.

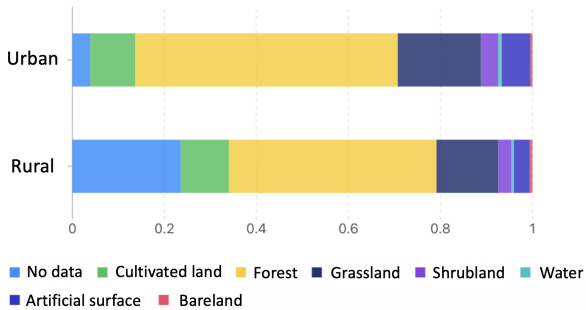


Figure 11. **Slovenia dataset class distribution shifts:** Class distribution for images from the two groups: urban, rural of the Slovenia dataset.

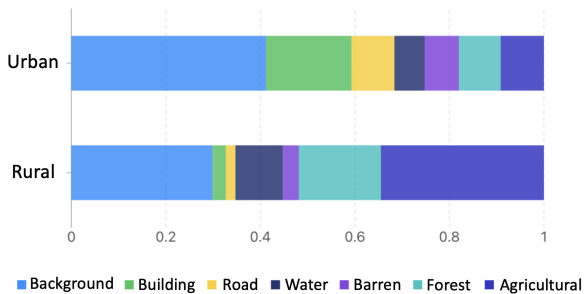


Figure 12. **LoveDA dataset class distribution shifts:** Class distribution for images from the two groups: urban, rural of the LoveDA dataset.

Layer	Input	Output
1×1 Conv2D (514, 514)	514	514
1×1 Conv2D (514, 50)	514	50
1×1 Conv2D (50, 1)	50	1

Table 6. Discriminator for layer2 of ResNet50 encoder.

ture map pair respectively. Details of building feature map pairs are described in Section 4 and visualized in Figure 5. As the next step, the discriminator outputs are used to com-

Layer	Input	Output
1×1 Conv2D (1026, 1026)	1026	1026
1×1 Conv2D (1026, 100)	1026	100
1×1 Conv2D (100, 1)	100	1

Table 7. Discriminator for layer3 of ResNet50 encoder.

Layer	Input	Output
1×1 Conv2D (2050, 2050)	2050	2050
1×1 Conv2D (2050, 200)	2050	200
1×1 Conv2D (200, 1)	200	1

Table 8. Discriminator for layer4 of ResNet50 encoder.

pute the mutual information estimation MI_{JSD}^4 and the discriminator loss \mathcal{L}_{D_i} listed in Section 4.

D. Supplementary experiment results

In Table 9, we provide standard deviation results of the 5 independent runs for the results shown in Table 1.

In Table 10, we generalize FairDCL and the comparison fair representation learning methods to a different contrastive pre-training framework DenseCL [63]. The same metrics are reported as with MoCo-v2 framework.

In Figure 13, different to how we have been defining the fairness-accuracy trade-off with the fairness metric: the group difference, which is more commonly used to quantify disparity, we further depict the trade-off with regard to another fairness metric: the worst-case performer.

We use pareto curve following [77], which assumes that computer vision models tend to have a capacity threshold, that a higher maximum group accuracy can lead to a lower minimum group accuracy, and vice versa, with the premise that the fairness intervention does not affect model’s efficiency. Under this assumption, the FairDCL method shows higher minimum group accuracy with the overall model accuracy least affected (Figure 13).

⁴Codes for the loss function are from <https://github.com/rdevon/DIM>

	Method	Iteration=1k			Iteration=2k			Iteration=3k			Iteration=4k			Iteration=5k		
		Diff	Wst	Acc												
LoveDA	Baseline	0.11	0.040	0.056	0.047	0.036	0.044	0.026	0.025	0.033	0.014	0.025	0.035	0.033	0.020	0.031
	GR	0.11	0.051	0.053	0.069	0.040	0.045	0.027	0.021	0.027	0.025	0.040	0.044	0.031	0.011	0.025
	DI	0.057	0.076	0.094	0.029	0.021	0.034	0.064	0.037	0.039	0.023	0.033	0.048	0.025	0.017	0.038
	UnbiasedR	0.078	0.095	0.066	0.022	0.022	0.039	0.052	0.049	0.030	0.019	0.039	0.035	0.024	0.037	0.028
	FairDCL	0.054	0.034	0.059	0.031	0.023	0.034	0.012	0.023	0.029	0.006	0.013	0.031	0.029	0.027	0.035
Slovenia	Baseline	0.065	0.015	0.026	0.062	0.012	0.022	0.093	0.020	0.023	0.065	0.010	0.019	0.051	0.007	0.015
	GR	0.041	0.012	0.024	0.069	0.022	0.029	0.073	0.021	0.026	0.062	0.023	0.034	0.077	0.006	0.024
	DI	0.011	0.019	0.024	0.059	0.006	0.019	0.015	0.012	0.018	0.079	0.011	0.022	0.074	0.013	0.023
	UnbiasedR	0.021	0.033	0.045	0.062	0.106	0.029	0.017	0.051	0.040	0.035	0.018	0.022	0.064	0.033	0.019
	FairDCL	0.020	0.008	0.021	0.057	0.009	0.021	0.007	0.010	0.022	0.029	0.012	0.020	0.054	0.004	0.020
CityScapes	Baseline	0.009	0.032	0.032	0.002	0.014	0.020	0.005	0.040	0.047	0.005	0.014	0.024	0.005	0.016	
	GR	0.002	0.009	0.016	0.005	0.027	0.030	0.008	0.045	0.046	0.003	0.011	0.018	0.004	0.007	0.019
	DI	0.002	0.013	0.020	0.003	0.046	0.049	0.005	0.028	0.030	0.010	0.045	0.042	0.004	0.007	0.015
	UnbiasedR	0.009	0.019	0.030	0.003	0.035	0.051	0.004	0.037	0.032	0.008	0.025	0.026	0.002	0.019	0.018
	FairDCL	0.006	0.020	0.027	0.002	0.027	0.029	0.006	0.010	0.020	0.002	0.016	0.021	0.004	0.011	0.019

Table 9. **Standard deviation** of results in Table 1. The smallest deviation results are marked in bold between the comparison methods for each iteration. It shows that FairDCL method produces comparable performance consistency from run to run with the baseline methods.

Method	Iteration=1k			Iteration=2k			Iteration=3k			Iteration=4k			Iteration=5k			No TO	
	Diff(↓)	Wst (↑)	Acc(↑)	Diff(↓)	Wst(↑)	Acc(↑)	Diff(↓)	Wst(↑)	Acc(↑)	Diff(↓)	Wst(↑)	Acc(↑)	Diff(↓)	Wst(↑)	Acc(↑)		
Baseline	0.204	0.308	0.339	0.089	0.358	0.374	0.118	0.388	0.411	0.116	0.399	0.422	0.103	0.383	0.403		
GR	0.170	0.326	0.354	0.104	0.365	0.384	0.114	0.369	0.390	0.110	0.406	0.428	0.092	0.388	0.406	✓	
DI	0.187	0.308	0.321	0.048	0.347	0.351	0.089	0.369	0.386	0.097	0.388	0.406	0.088	0.366	0.383	✗	
UnbiasedR	0.169	0.299	0.324	0.116	0.380	0.402	0.087	0.386	0.403	0.095	0.396	0.415	0.90	0.386	0.403	✗	
FairDCL	0.168	0.336	0.365	0.076	0.385	0.399	0.108	0.394	0.415	0.091	0.406	0.43	0.083	0.391	0.408	✓	
	Iteration=6k			Iteration=7k			Iteration=8k			Iteration=9k			Iteration=10k				
	Baseline	0.102	0.401	0.421	0.085	0.421	0.329	0.077	0.435	0.452	0.087	0.434	0.453	0.106	0.424	0.446	
	GR	0.094	0.402	0.421	0.081	0.420	0.437	0.083	0.441	0.459	0.099	0.431	0.452	0.106	0.425	0.448	✗
	DI	0.087	0.389	0.405	0.082	0.414	0.424	0.087	0.420	0.436	0.085	0.422	0.435	0.108	0.420	0.441	✗
	UnbiasedR	0.086	0.401	0.419	0.092	0.416	0.435	0.098	0.408	0.428	0.092	0.431	0.451	0.104	0.424	0.445	✗
FairDCL	0.084	0.405	0.422	0.080	0.423	0.440	0.074	0.445	0.461	0.083	0.435	0.453	0.104	0.428	0.452	✓	

Table 10. **Testing the generalizability to the different contrastive pre-training framework DenseCL**. We run 10k fine-tuning iterations on the downstream semantic segmentation on LoveDA dataset. Similarly, the frozen encoder weights are learnt with different fairness method: Baseline (no intervention), GR, DI, UnbiasedR, and our FairDCL. For every 1k steps, the best results in term of fairness: group difference (Diff) and worst-case group result (Wst), and accuracy: mean IoU (Acc) are marked in bold. The fairness-accuracy trade-off indicator (No TO) shows whether a method, in its best performing round, obtains both better Diff and Wst than the Baseline (✓) or fails to do so (✗). **FairDCL** continuously shows supreme fairness performance on this alternative contrastive learning pipeline, and avoids the undesired trade-off throughout the fine-tuning.

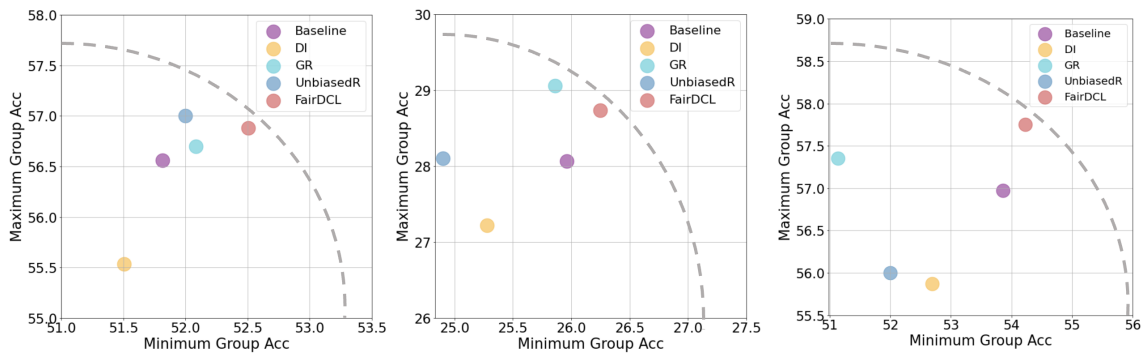


Figure 13. **Worst case group - Accuracy trade-off depiction:** For each colored dot, a closer distance to the grey dotted curve (maximum model capacity) indicates a higher model efficiency in term of overall accuracy. A larger x-axis value indicates the model is fairer and has a higher minimum group accuracy. The plots are for results on LoveDA (left), Slovenia (middle), and CityScapes (right) dataset. FairDCL shows better fairness performances on the worst case group's aspect meanwhile a higher and stable model efficiency.